Ground-based, integrated path differential absorption LIDAR measurement of CO_2, CH_4, and H_2O near 1.6 μm

Supplemental

GERD A. WAGNER[1] AND DAVID F. PLUSQUELLIC[1,*]

[1] *Quantum Electromagnetics Division, Physical Measurement Laboratory, National Institute of Standards and Technology, Boulder, Colorado 80305, USA*
[*] *Corresponding author: david.plusquellic@nist.gov*

Compiled August 8, 2016

Supplementary material to Applied Optics 55(23), 6292-6310 (2016), http://dx.doi.org/10.1364/AO.55.006292
Version of 8/8/2016 01:51 PM (MST)

OCIS codes: *(280.1910) DIAL, differential absorption lidar; (280.3640) Lidar.*

http://doi.org/10.18434/T49W2V

SUPPLEMENTARY MATERIAL

- PMT dark counts versus PMT box temperature: this document, Figure 1 .
- Overview of measurements: this document, Table 1.
- IPDA LIDAR: data are available in NetCDF file format at http://doi.org/10.18434/T49W2V .
- Aerosol backscatter LIDAR: data are available in NetCDF file format at http://doi.org/10.18434/T49W2V .
- CRD sensor (Picarro G2301): data are available in NetCDF file format at http://doi.org/10.18434/T49W2V .
- Weather sensor (Vaisala WXT520): data are available in NetCDF file format at http://doi.org/10.18434/T49W2V .
- Thorlabs temperature sensor (TSP01): data are available in NetCDF file format at http://doi.org/10.18434/T49W2V .

REFERENCES

1. Certain equipment, instruments or materials are identified in this paper in order to adequately specify the experimental details. Such identification does not imply recommendation by the National Institute of Standards and Technology nor does it imply the materials are necessarily the best available for the purpose.
2. K. O. Douglass, S. E. Maxwell, G.-W. Truong, R. D. van Zee, J. R. Whetstone, J. T. Hodges, D. A. Long, and D. F. Plusquellic, "Rapid scan absorption spectroscopy using a waveform-driven electro-optic phase modulator in the 1.6-1.65 μm region," JOSA B **30**, 2696–2703 (2013).
3. K. O. Douglass, S. E. Maxwell, D. A. Long, J. T. Hodges, and D. F. Plusquellic, "Fast switching arbitrary frequency light source for broadband spectroscopic applications," U.S. patent 13/827,476 (March 14, 2013).
4. G. Wagner, S. Maxwell, and D. Plusquellic, "Integrated path detection of CH_4 and CO_2 using a waveform driven electro-optic single sideband laser source," in Proceedings of the 27th International Laser and Radar Conference (ILRC), New York, USA, 5-10 July, paper S13-02, 2015, EPJ Web of Conferences 119, 26002 (2016), http://dx.doi.org/10.1051/epjconf/201611926002 .
5. G. A. Wagner and D. F. Plusquellic, "Ground-based, integrated path differential absorption LIDAR measurement of CO_2, CH_4, and H_2O near 1.6 μm," Appl. Opt. **55**, 6292–6310 (2016).
6. G. A. Wagner and D. F. Plusquellic, "Ground-based, integrated path differential absorption LIDAR measurement of CO_2, CH_4, and H_2O near 1.6 μm - Supplemental," http://doi.org/10.18434/T49W2V .

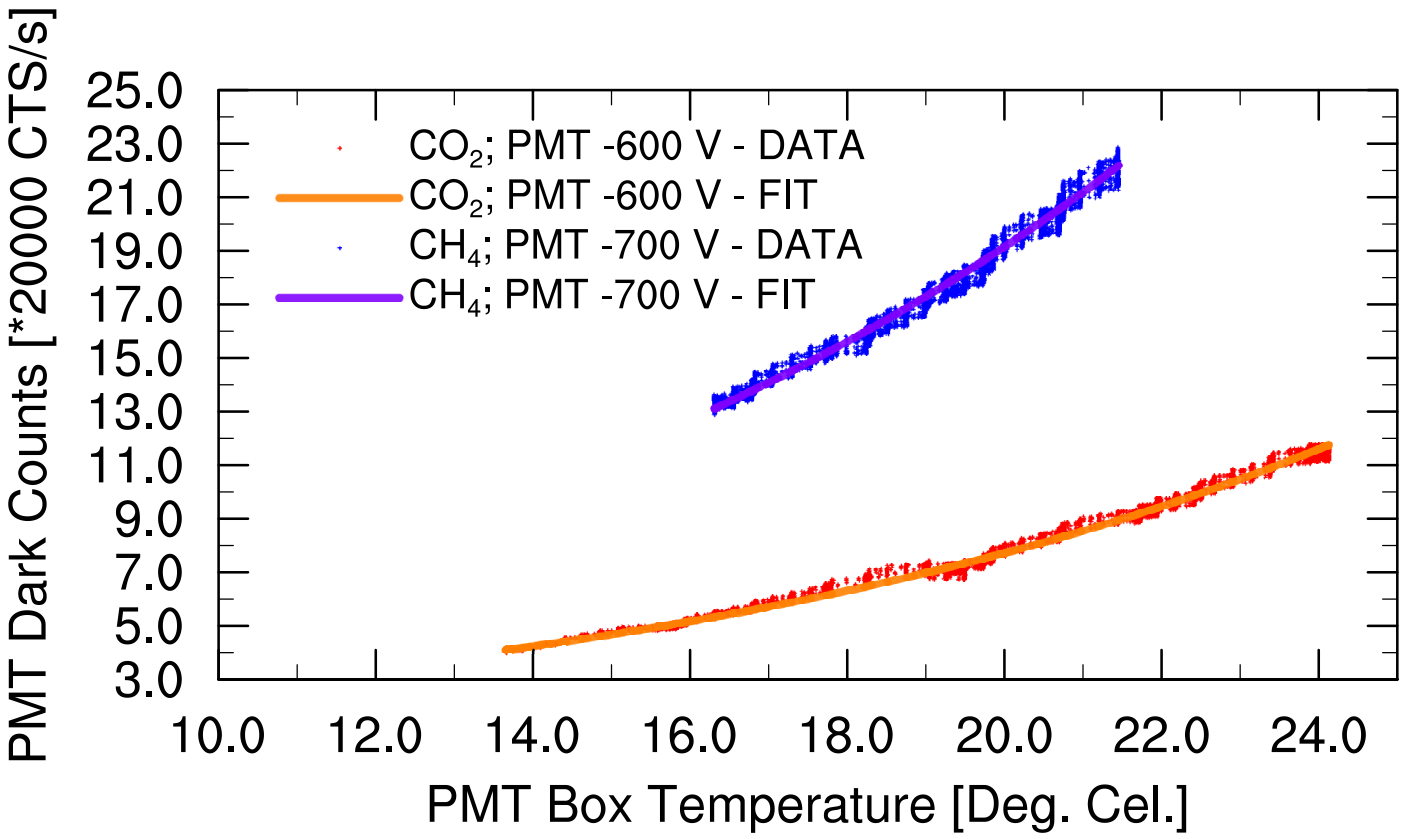

Fig. 1. PMT dark counts as a function of PMT box temperature for CO_2 (-600 V) and CH_4 (-700 V) measurement configuration. FIT (CO_2): $f(x) = 0.92077 * exp(0.10467 * x) + 0.25927$; FIT ($CH_4$): $g(x) = 2.8518 * exp(0.097403 * x) - 0.84751$.

Table 1. Overview of measurements [1] and availability of raw data at http://doi.org/10.18434/T49W2V.

Date (UTC)	Detected Species	Overview Figure	IPDA LIDAR DATA	BS LIDAR DATA	Picarro G2301 DATA	Vaisala WXT520 DATA	Thorlabs TSP01 DATA
Oct. 09, 2015	CO_2, H_20	2	yes	yes	yes	yes	yes
Oct. 10, 2015	CO_2, H_20	3	yes	yes	yes	yes	yes
Oct. 11, 2015	CO_2, H_20	4	yes	yes	yes	yes	yes
Oct. 12, 2015	CO_2, H_20	5	yes	yes	yes	yes	yes
Oct. 13, 2015	CO_2, H_20	6	yes	yes	yes	yes	yes
Oct. 14, 2015	CO_2, H_20	7	yes	yes	yes	yes	yes
Oct. 15, 2015	CH_4, H_20	8	yes	yes	yes	yes	yes
Oct. 16, 2015	CH_4, H_20	9	yes	yes	yes	yes	yes
Oct. 17, 2015	CH_4, H_20	10	yes	yes	yes	yes	yes
Oct. 18, 2015	CH_4, H_20	11	yes	yes	yes	yes	yes
Oct. 19, 2015	CH_4, H_20	12	yes	yes	yes	yes	yes

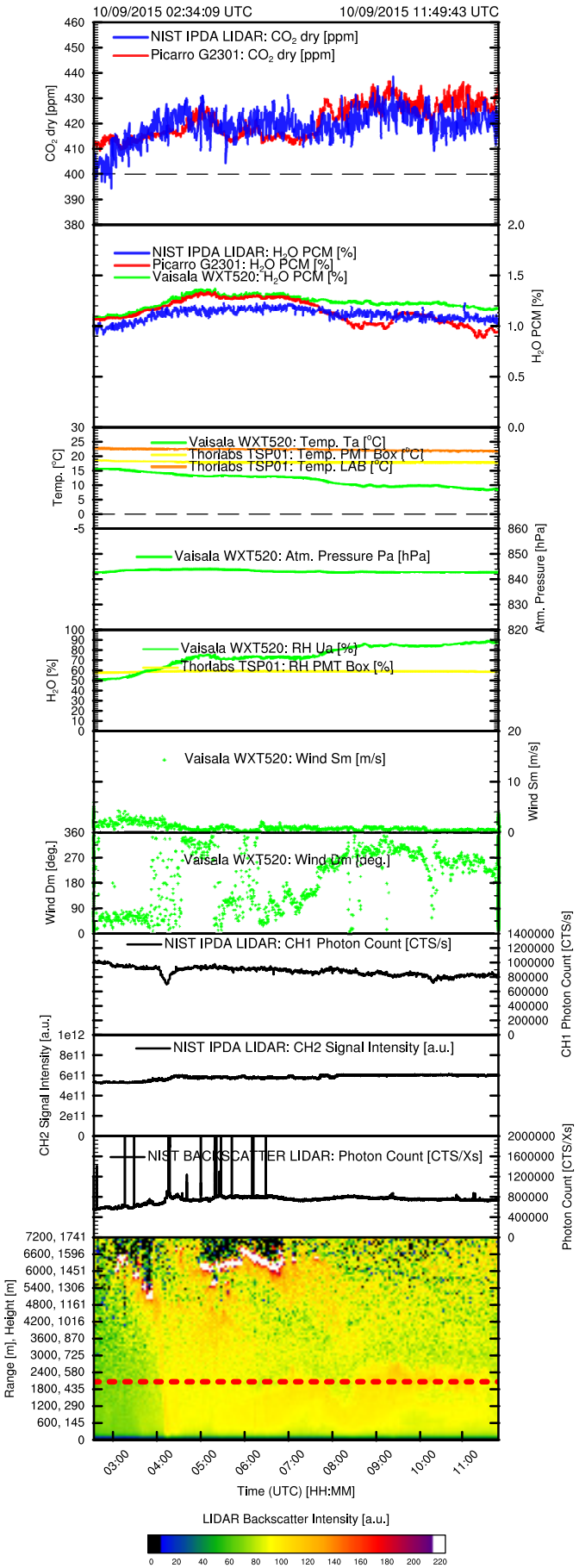

Fig. 2. IPDA LIDAR CO_2 dry concentrations in μmol/mol (ppm) on October 09, 2015.

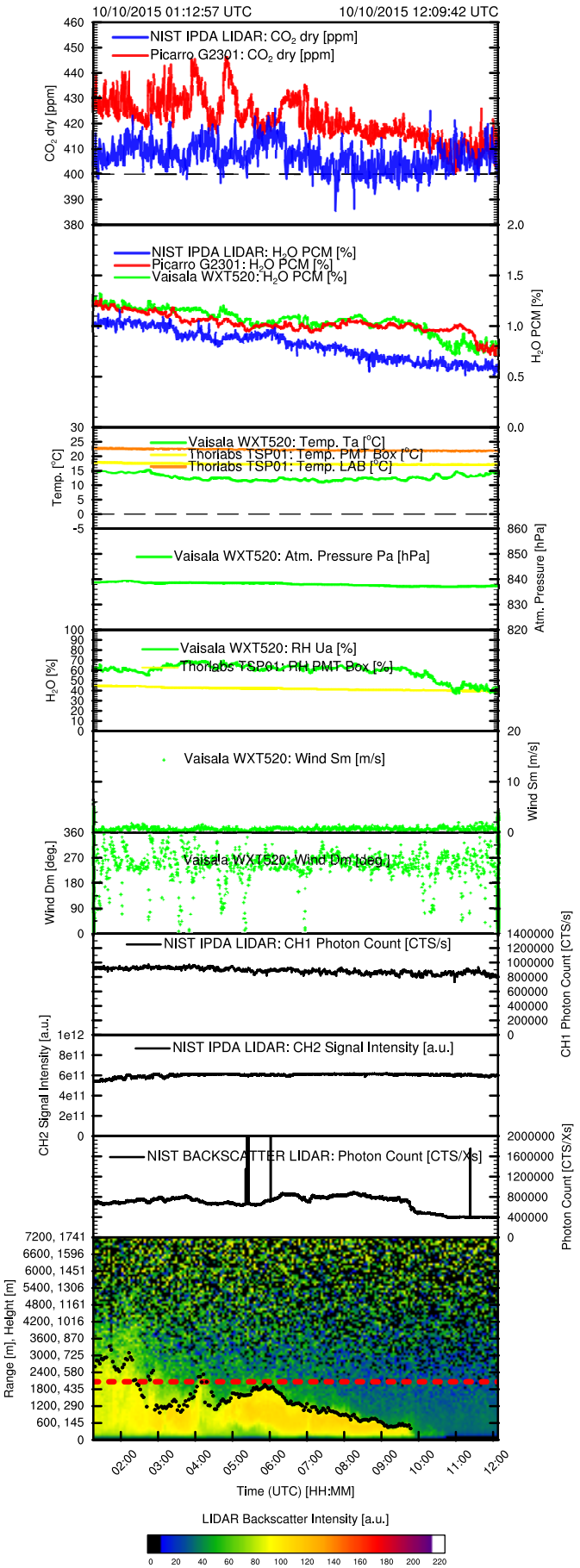

Fig. 3. IPDA LIDAR CO_2 dry concentrations in μmol/mol (ppm) on October 10, 2015.

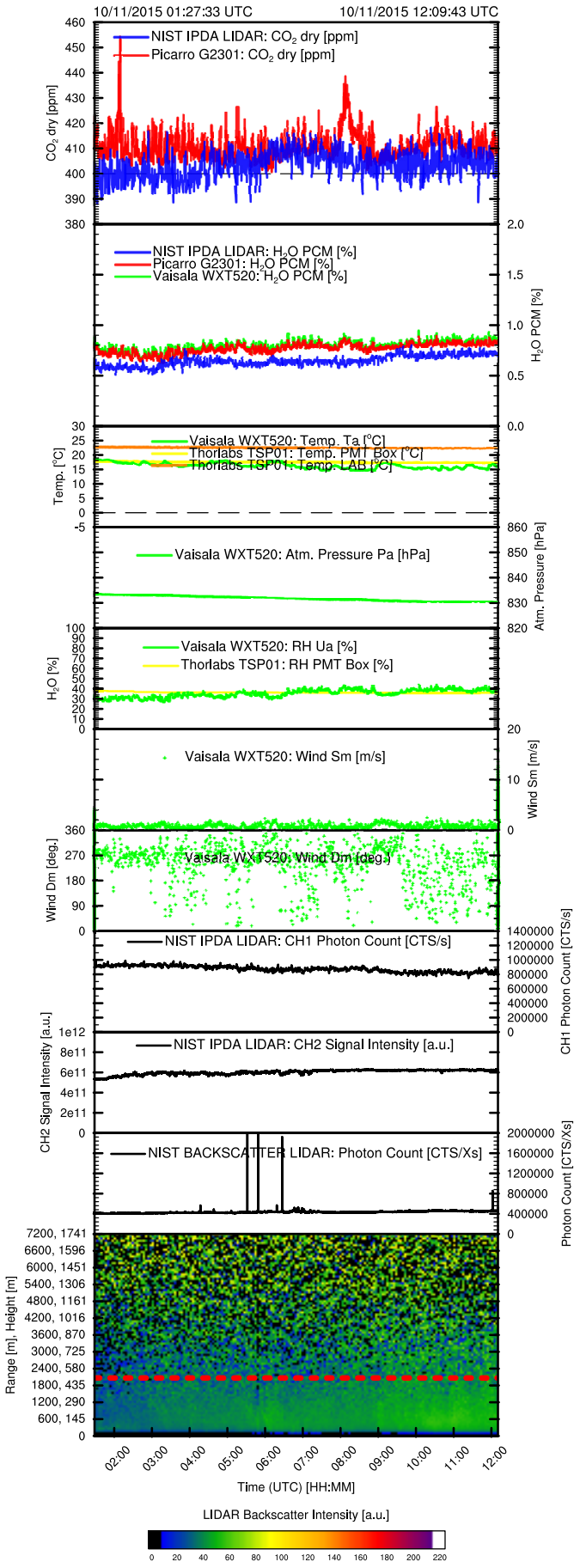

Fig. 4. IPDA LIDAR CO_2 dry concentrations in μmol/mol (ppm) on October 11, 2015.

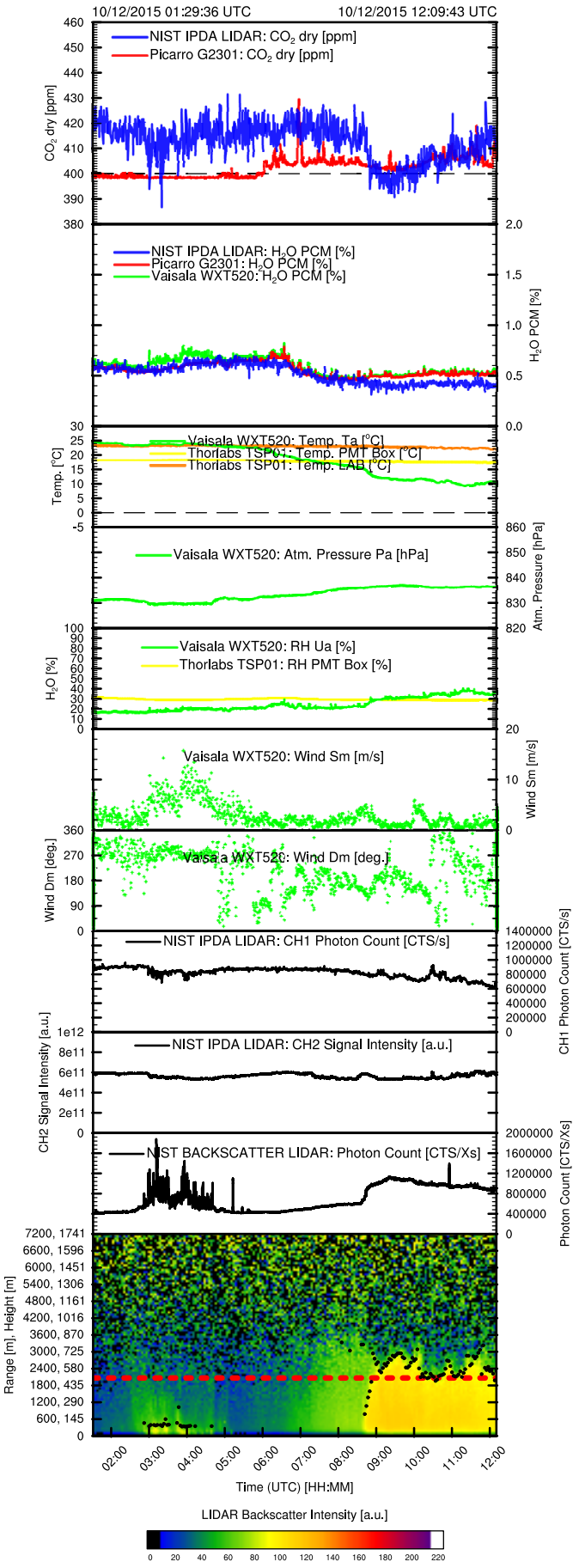

Fig. 5. IPDA LIDAR CO_2 dry concentrations in μmol/mol (ppm) on October 12, 2015.

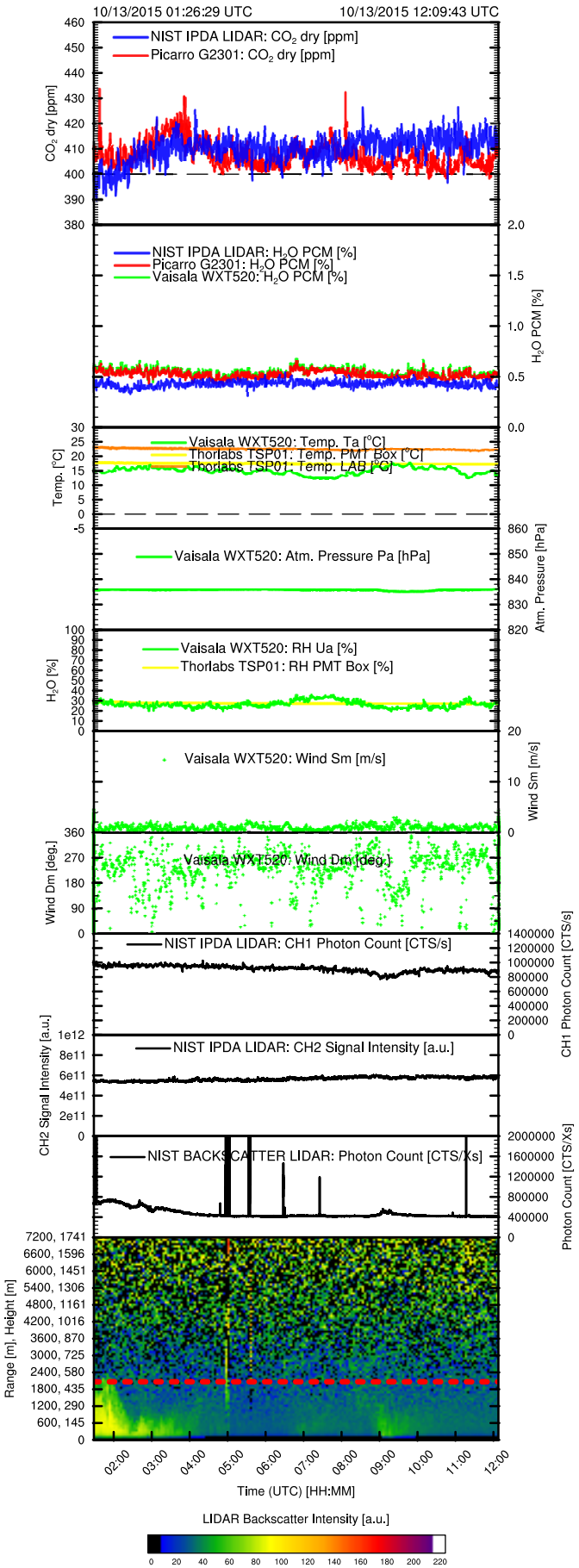

Fig. 6. IPDA LIDAR CO_2 dry concentrations in μmol/mol (ppm) on October 13, 2015.

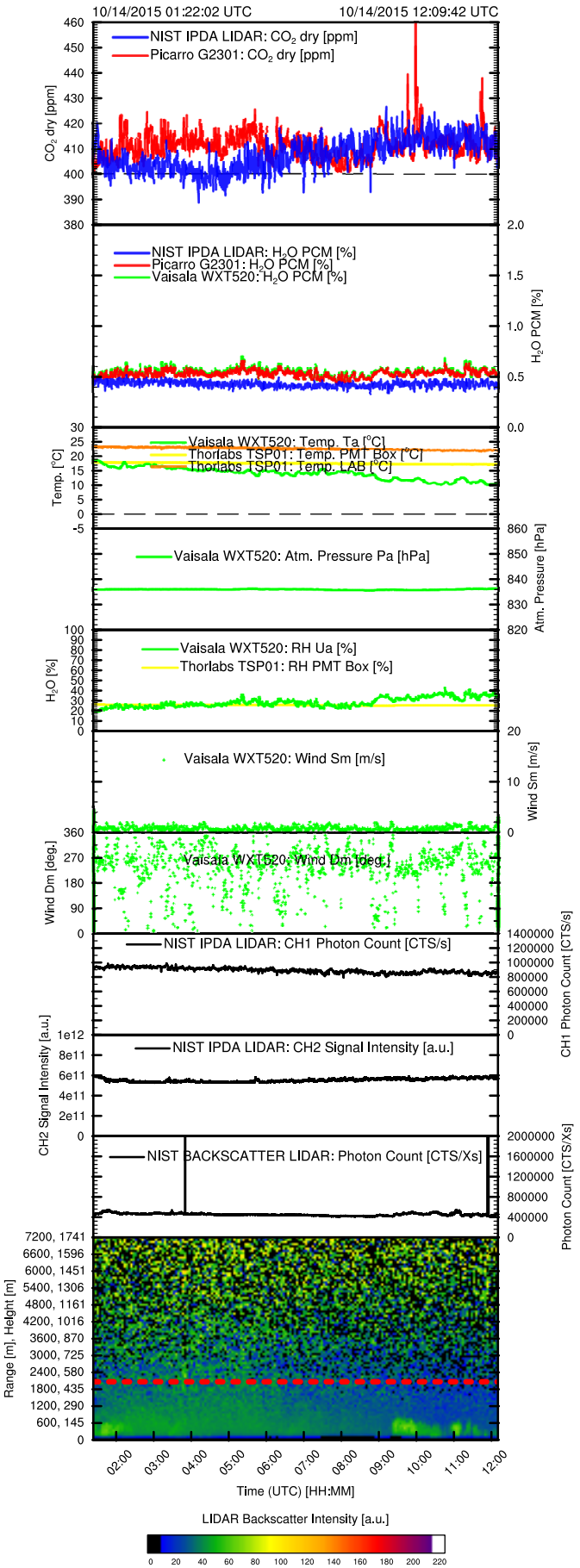

Fig. 7. IPDA LIDAR CO_2 dry concentrations in μmol/mol (ppm) on October 14, 2015.

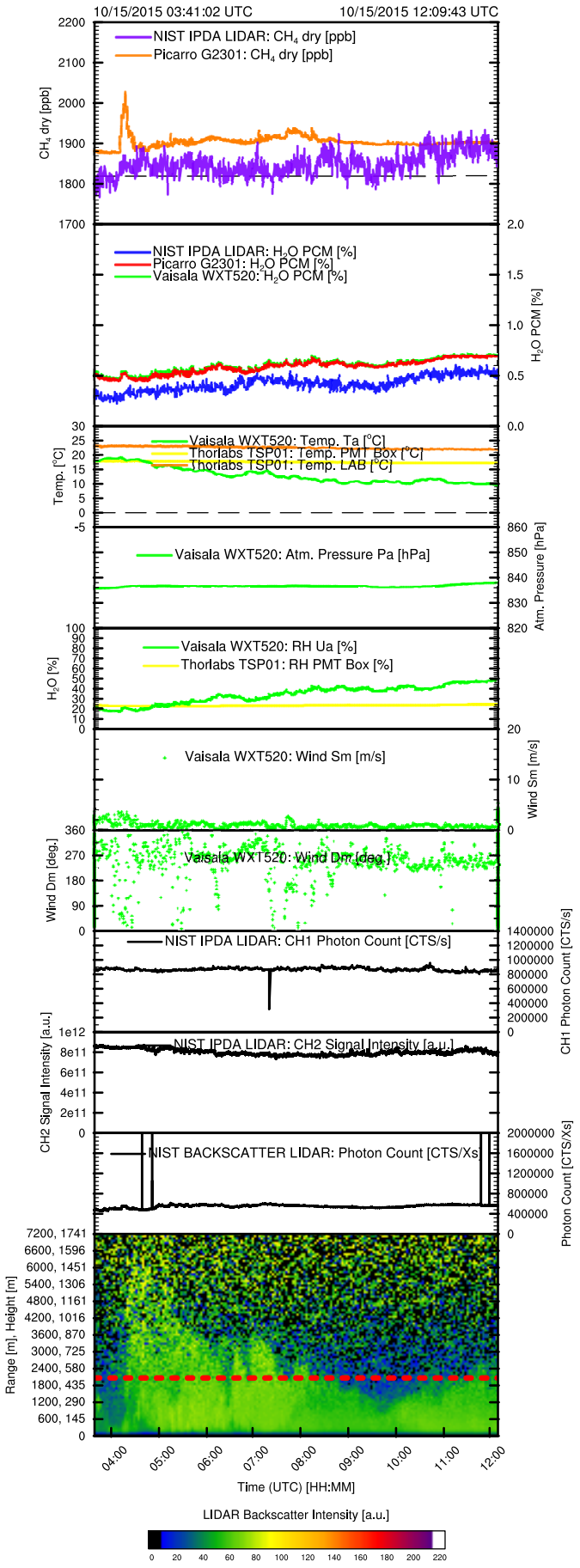

Fig. 8. IPDA LIDAR CH_4 dry concentrations in nmol/mol (ppb) on October 15, 2015.

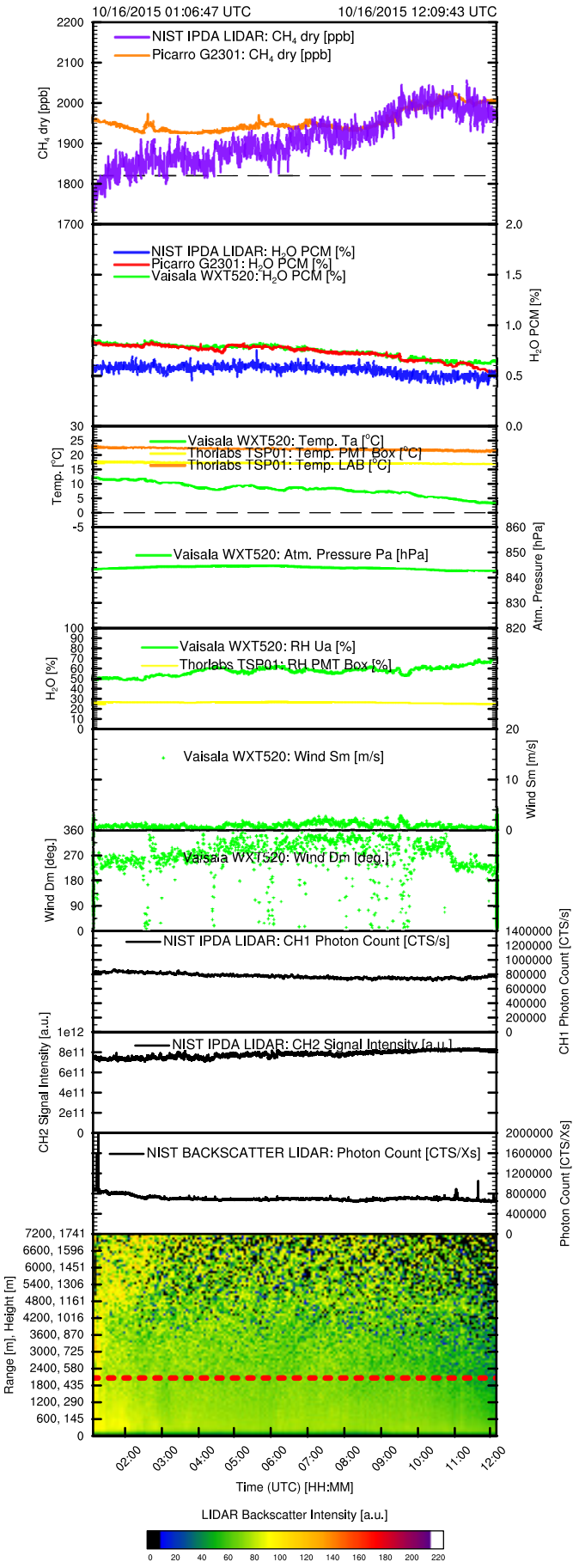

Fig. 9. IPDA LIDAR CH_4 dry concentrations in nmol/mol (ppb) on October 16, 2015.

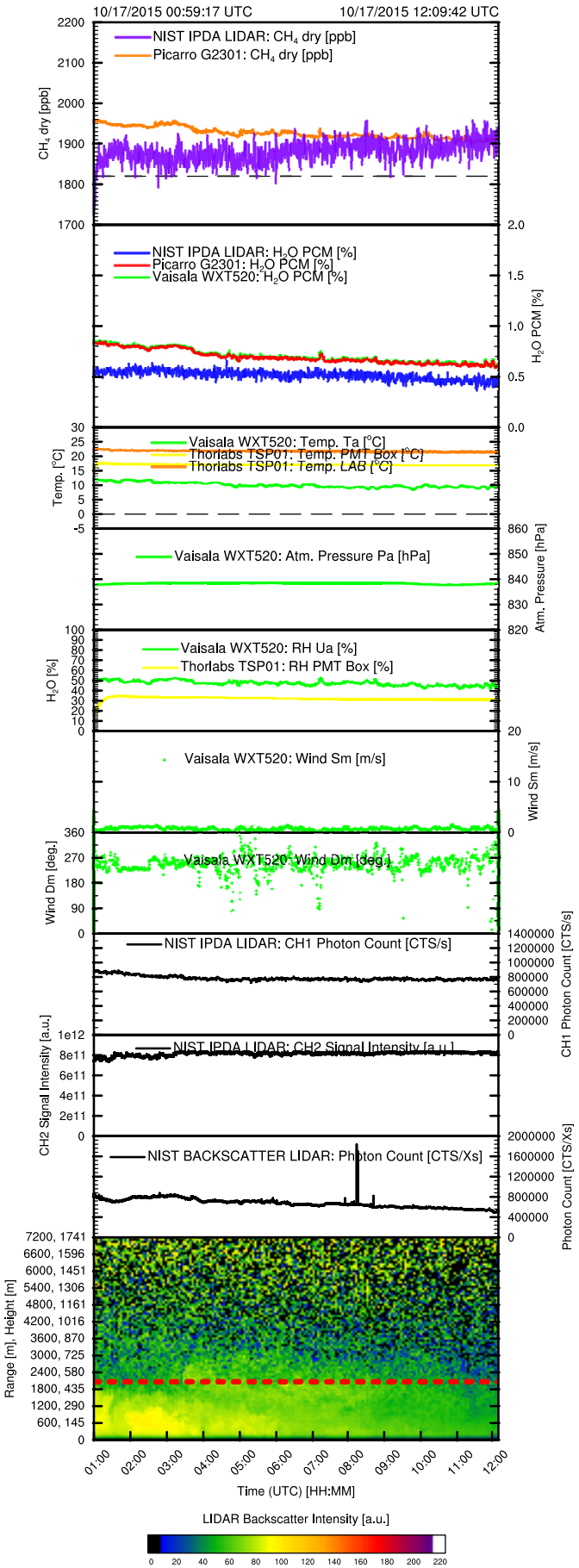

Fig. 10. IPDA LIDAR CH_4 dry concentrations in nmol/mol (ppb) on October 17, 2015.

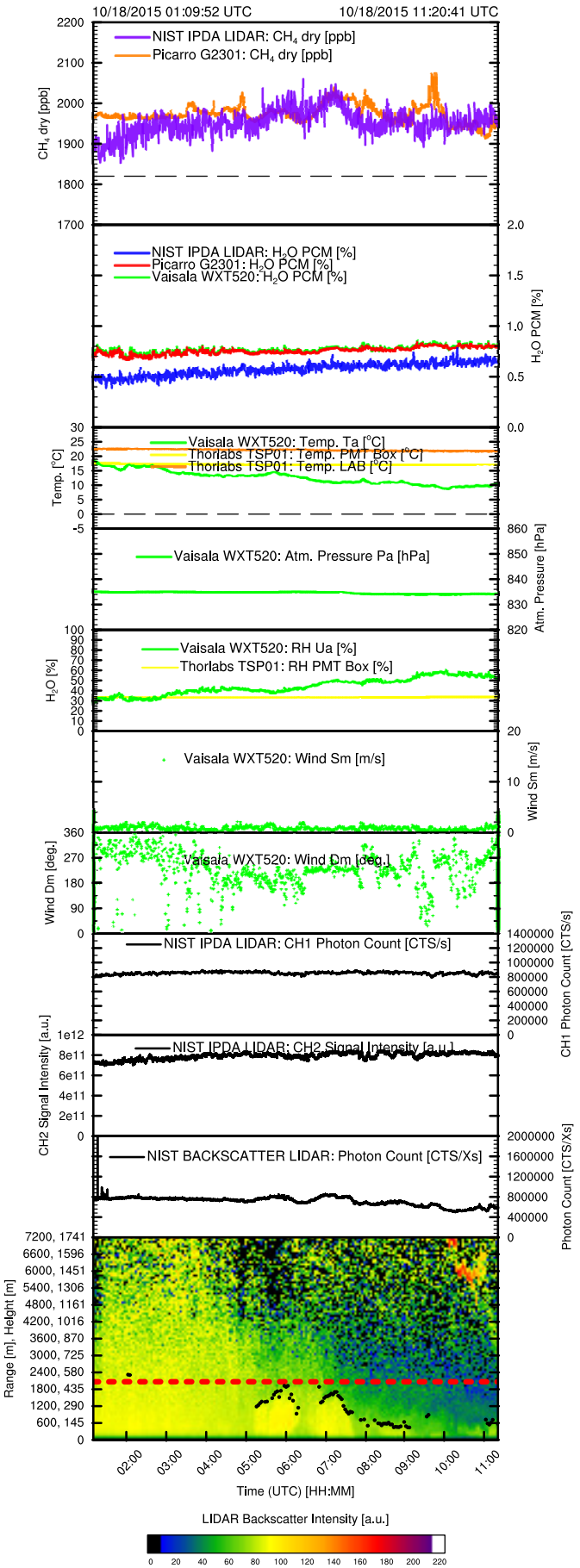

Fig. 11. IPDA LIDAR CH_4 dry concentrations in nmol/mol (ppb) on October 18, 2015.

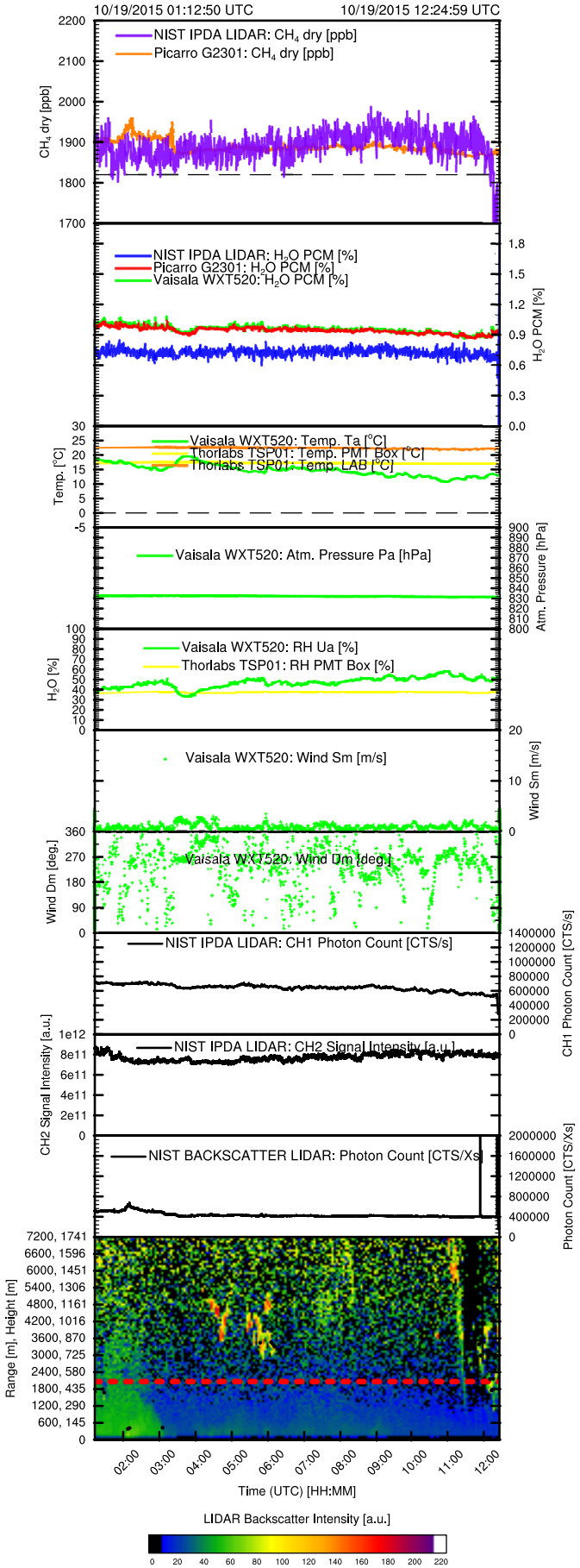

Fig. 12. IPDA LIDAR CH_4 dry concentrations in nmol/mol (ppb) on October 19, 2015.